

AperTO - Archivio Istituzionale Open Access dell'Università di Torino

Enhanced CO₂ adsorption capacity of amine-functionalized MIL-100(Cr) metal-organic frameworks

This is the author's manuscript

Original Citation:

Availability:

This version is available <http://hdl.handle.net/2318/1506325> since 2016-10-03T11:29:06Z

Published version:

DOI:10.1039/c4ce01265h

Terms of use:

Open Access

Anyone can freely access the full text of works made available as "Open Access". Works made available under a Creative Commons license can be used according to the terms and conditions of said license. Use of all other works requires consent of the right holder (author or publisher) if not exempted from copyright protection by the applicable law.

(Article begins on next page)



UNIVERSITÀ DEGLI STUDI DI TORINO

This is an author version of the contribution published on:

Carlos Palomino Cabello, Gloria Berlier, Giuliana Magnacca, Paolo
Rumori, Gemma Turnes Palomino
Enhanced CO₂ adsorption capacity of amine-functionalized MIL-100(Cr)
metal-organic frameworks
CRYSTENGCOMM (2015) 17
DOI: 10.1039/C4CE01265H

The definitive version is available at:
<http://xlink.rsc.org/?DOI=C4CE01265H>

Enhanced CO₂ adsorption capacity of amine-functionalized MIL-100(Cr) metal-organic frameworks

Carlos Palomino Cabello,^a Gloria Berlier,^b Giuliana Magnacca,^b Paolo Rumori^a and Gemma Turnes Palomino^{a,*}

^a *Department of Chemistry, University of the Balearic Islands, 07122 Palma de Mallorca, Spain. Tel.: (+34)-971-173250; Fax: (+34)-971-173426; E-mail: g.turnes@uib.es*

^b *University of Torino, Department of Chemistry and NIS Centre, Via P.Giuria 7, 10125 Torino, Italy*

Amine-functionalized metal-organic frameworks, EN-MIL-100(Cr) and MMEN-MIL-100(Cr), were prepared by grafting ethylenediamine and N,N'-dimethylethylenediamine molecules, respectively, on coordinatively unsaturated chromium(III) cations in MIL-100 metal-organic frameworks. Although amine grafting results in a decrease of surface area and pore volume of the functionalized samples compared to the bare MIL-100(Cr), results showed that the incorporation of amine groups into the MIL-100 framework improve both carbon dioxide adsorption capacity and kinetics, especially in the case of ethylenediamine. Heats of carbon dioxide adsorption in EN-MIL-100(Cr) and MMEN-MIL-100(Cr) were of about 80 kJ mol⁻¹ at zero coverage, a value higher than that shown by MIL-100(Cr), which suggests a chemisorption between CO₂ and pendant amine groups. Measurement of CO₂ adsorption-desorption cycles proved that functionalized materials show good regenerability and stability.

Introduction

Over 80% of our current global energy demand is satisfied by burning fossil fuels which releases large amounts of CO₂ into the atmosphere.¹ The consequent increase of greenhouse effect, which can adversely affect climate, is causing worldwide concern. Replacing fossil fuels with renewable, and cleaner, energy sources could provide a way out of this problem in the long run, but we still need a mid-term solution to allow the humanity to continue using fossil fuels until cost-effective renewable energy can be implemented on a large scale.² Carbon dioxide capture and sequestration (CCS) could constitute part of that mid-term solution, particularly if current research in this area brings about a significant reduction of cost.³⁻⁷

Current technology for CCS uses mainly liquid amine-based chemical absorbents,^{8,9} but besides the high amount of energy required for regenerating the sorbent,^{10,11} that technology poses some corrosion problems and environmental hazards derived from waste processing, unintentional

emissions and accidental release.^{12,13} To overcome the drawbacks of amine aqueous solutions, several types of porous adsorbents that can reversibly capture and release CO₂ (in temperature- or pressure-swing cycles) are currently under active investigation as a means to facilitate CO₂ capture from flue gases of stationary sources.¹⁴⁻¹⁸

Metal-Organic Frameworks (MOFs) have emerged as promising adsorbent materials for CO₂ capture due to their high surface area, large pore volume and tunable pore surface.¹⁹⁻²² The ability to design and tune the properties of MOFs makes these adsorbent materials distinct from other traditional adsorbents such as zeolites and carbon materials.²³⁻²⁸ For effective CO₂ capture from flue gas, both high CO₂ capacity and high CO₂ selectivity are requisite attributes of the MOF adsorbents. While various strategies have been studied to improve CO₂ adsorption in MOFs, three approaches proved to be particularly effective: incorporation of unsaturated metal cation centers, metal doping and chemical functionalization.²⁸ Among them, the incorporation of pendant alkylamine functionalities within the pores of metal-organic frameworks seems to be a promising strategy for increasing the capacity and selectivity of metal-organic frameworks for CO₂ uptake by virtue of the affinity of alkylamines for CO₂.²⁹⁻⁴⁰ Two major strategies are envisaged to achieve this goal: (i) the direct use of an amine-based bridging ligands to generate the three-dimensional network,^{29,30,32} or (ii) postsynthetic approaches that covalently modify a bridging ligand or graft an alkylamine functionality onto a coordinatively unsaturated metal center.^{31,33-40} This last approach has been used by different authors during the last years resulting generally in an improvement of CO₂ selectivity and an enhancement in CO₂ capacity, especially at low pressures.

However, for MOFs to be practically useful as adsorbents for either CO₂ capture from flue gas or natural gas upgrading, a number of aspects need to be carefully evaluated in addition to capacity and selectivity. Chemical and thermal stability are also two very important parameters for MOFs to be considered for CO₂ adsorption. While many MOFs are hydrolytically unstable,²⁶ there are a number of MOFs which have high chemical and thermal stability. Some of the most well-known examples include those generated from either high-valency metal ions such as Al³⁺ (Al-MIL-110), Cr³⁺ (Cr-MIL-101 and Cr-MIL-100) and Zr⁴⁺ (UiO-66) or various nitrogen-donor ligands containing imidazole (ZIFs), pyrazole, triazole, and tetrazole.²⁸ Among them, the MIL-100⁴¹⁻⁴³ and MIL-101⁴⁴⁻⁴⁷ families, originally developed by Ferey's group, has a great potential due to a large surface area, high pore volume, numerous potential unsaturated chromium sites, and high thermal and chemical stability.

MIL-100(Cr) is a MOF that has the chemical composition $\text{Cr}_3\text{O}(\text{F}/\text{OH})(\text{H}_2\text{O})_2[\text{C}_6\text{H}_3(\text{CO}_2)_3]_2 \cdot n\text{H}_2\text{O}$ and which is known to exhibit very high air, water, and thermal stability compared to other MOFs, maintaining its structural integrity even after prolonged immersion in water.^{42,43} It is a chromium(III) carboxylate built from trimers of metal octahedra sharing a common oxygen atom which are linked together by trimesate rigid ligands. After solvent removal, the framework structure (which is cubic) shows two types of empty mesoporous cages having free apertures of approx. 2.9 and 3.4 nm, accessible through microporous windows of approx. 0.55 and 0.86 nm, respectively.⁴¹ There is also a terminal H_2O ligand that can be removed by appropriate thermal treatment, to leave an open (coordinatively unsaturated) cationic site to which diamine molecules can be grafted through one of the amine groups, so that the second amine group remains available as a chemically reactive adsorption site (Figure 1). Following this strategy, we report on the postsynthesis amine functionalization of a MIL-100(Cr) MOF and show that the incorporation of amine groups in the framework leads to sorbent materials with improved CO_2 adsorption capacity, fast carbon dioxide adsorption-desorption kinetics as well as very good stability over multiple adsorption-desorption cycles.

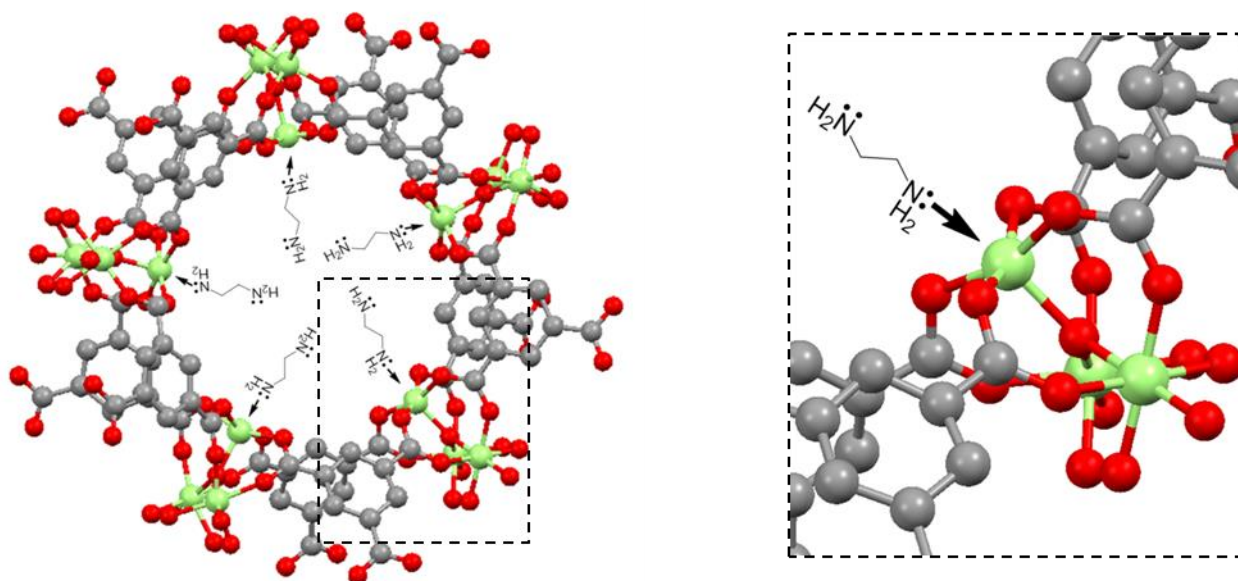


Fig. 1 Schematic representation of the MIL-100(Cr) framework. The inset shows the mode of coordination of an ethylenediamine molecule to a coordinatively unsaturated chromium ion. Metal, carbon and oxygen atoms are depicted as green, gray and red spheres, respectively.

Experimental section

Synthesis of MIL-100(Cr) The MIL-100(Cr) sample used was prepared by a hydrothermal reaction following the procedure described by Férey et al.^{41,48} in which 4.95 mmol of chromium trioxide (Sigma-Aldrich, 99%), 4.75 mmol of trimesic acid (Aldrich, 95%), 5 mmol of hydrofluoric acid (Fluka, 40%) and 24 ml of deionized water were mixed in a Teflon-lined stainless steel autoclave and kept at 493 K for 96 h. The resulting green solid was washed with deionized water and acetone (Scharlau, 99.5%) and dried at room temperature under air atmosphere.

Post-synthetic modification of MIL-100(Cr) with amines

Alkylamine functionalization of the coordinatively unsaturated Cr(III) sites was carried out using a procedure analogous to that reported for MIL-101.⁴⁹ 0.5 g of MIL-100(Cr), activated at 453 K for 12 h under a nitrogen atmosphere, was suspended in 50 ml of anhydrous toluene (Sigma-Aldrich, 99.5%). To this suspension, an excess (6 mmol) of the corresponding amine (ethylenediamine (Fluka, 99.5%) or N,N'-dimethylethylenediamine (Aldrich, 99%)) was added, and the mixture was refluxed under N₂ for 12 h to facilitate the amine grafting. The resulting solid was collected by filtration and repeatedly washed with hexane (Sigma-Aldrich, 95%) to remove unreacted amine, and then dried at room temperature. Samples were stored under ambient conditions (average relative humidity of 50% and room temperature) over a period of at least six months. In order to check their stability, the adsorption properties of the samples have been evaluated four times during this period following the procedure described in the following (vide infra).

Sample characterization

Powder X-ray diffraction data were collected using CuK α ($\lambda = 1.54056 \text{ \AA}$) radiation on a Siemens D5000 diffractometer.

Fourier transform infrared (FTIR) spectra were recorded on a Bruker IFS66 spectrometer, working at 3 cm⁻¹ resolution. For IR measurements, a thin, self-supported wafer of the MOF sample was prepared and activated (degassed) inside the IR cell under a dynamic vacuum (residual pressure < 10⁻⁴ mbar) at 453 K for 6 h. After this thermal treatment, carbon monoxide was dosed into the cell to check the presence of coordinative unsaturated chromium cations.

Elemental analysis was used to determine the nitrogen content and corresponding amine loading of the materials. The C, H, N, S content was determined using a Thermo Electron Corporation CHNS-O analyzer.

Nitrogen adsorption isotherms were measured at 77 K using a Micromeritics ASAP 2020 physisorption analyzer. All of the samples were outgassed at 423 K for 6 hours prior to measurement. Data were analysed using the Brunauer-Emmett-Teller (BET) model to determine the specific surface area. Pore volume and pore size distribution were calculated using the Barrett-Joyner-Halenda (BJH) method, applied to the nitrogen adsorption branch.

CO₂ sorption and cycling measurements

CO₂ adsorption was measured using a TA Instruments-SDT 2960 simultaneous DSC-TGA. Approximately 10 mg of each sample was heated from 298 to 373 K at 5 K min⁻¹ in N₂ atmosphere at a flow rate of 100 ml/min. The sample was held at 373 K for 90 min and then cooled to 308 K. Then the gas input was switched from N₂ to CO₂ and held isothermally at 308 K for 60 min. The CO₂ adsorption capacity was determined from the weight change of the sample after treatment with pure CO₂ (Air Products, 99.995%). Regenerability and multicycle stability was evaluated by repeating the above described procedure 15 times.

Microcalorimetric measurements

CO₂ heats of adsorption were determined according to a previously reported procedure^{50,51} by means of a Setaram Tian-Calvet-type instrument equipped with a gas-volumetric apparatus. CO₂ was contacted step by step with samples previously activated at 423 K for 6 hours and kept at 308 K during CO₂ adsorption measurements.

Results and discussion

The almost unchanged powder X-ray diffraction patterns after amine grafting (Figure 2) as compared to that of MIL-100(Cr) show that grafting occurs with no apparent loss of crystallinity, although a slight variation of the intensity of some of the diffraction peaks is observed. Amine grafting was confirmed by FTIR Spectroscopy. Figure 3 shows the spectrum of bare MIL-100(Cr) compared with the spectra of MIL-100(Cr) samples after ethylenediamine (EN-MIL-100(Cr)) and N,N'-dimethylethylenediamine (MMEN-MIL-100(Cr)) grafting; the spectra of pure ethylenediamine and N,N'-dimethylethylenediamine (in the liquid phase) are also shown for comparison. As

compared to MIL-100(Cr), EN-MIL-100(Cr) and MMEN-MIL-100(Cr) samples show additional absorption bands in the range of 3500 to 2800 cm^{-1} , also present in the pure amine spectra, which correspond to N-H and C-H stretching vibrations and confirm the presence of amine and methylene groups in the functionalized samples. Besides that, the corresponding $\nu(\text{C-H})$ IR absorption bands are shifted to larger wavenumbers compared with those of free amine molecules; as observed when the molecule is coordinated to a Lewis acid center,^{52,53} which prove selective amine grafting onto coordinatively unsaturated chromium cations in the two grafted-samples.

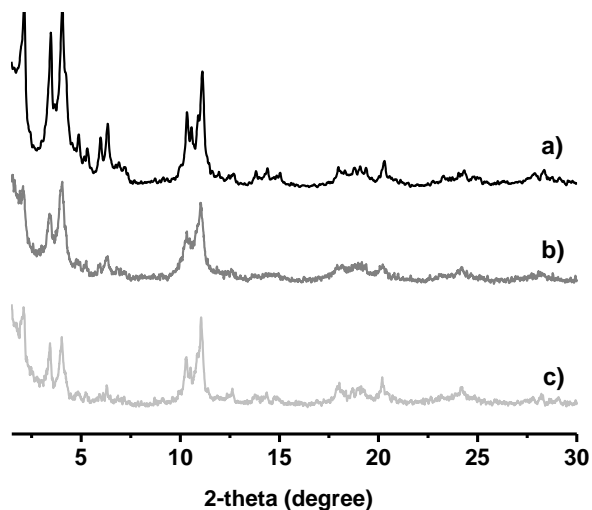


Fig. 2 X-ray diffractograms (CuK α radiation) of: a) MIL-100(Cr), b) MMEN-MIL-100(Cr), and c) EN-MIL-100(Cr).

Successful grafting of amine on open metal sites was also checked by FTIR spectroscopy of adsorbed carbon monoxide at 100 K. After thermal treatment of the samples at 453 K for 6 h, a saturation dose of carbon monoxide was introduced into the IR cell. The corresponding spectra are depicted in Figure 4. The IR spectrum of adsorbed CO on MIL-100(Cr) shows an intense IR absorption band, centred at 2194 cm^{-1} , which, in agreement with previous results by Férey et al.,⁴⁸ is assigned to the C=O stretching vibration of carbon monoxide adsorbed on the coordinatively unsaturated Cr(III) cations of MIL-100(Cr). After CO admission on EN-MIL-100(Cr) no band is observed at 2194 cm^{-1} , demonstrating the amine grafting onto open metal sites. In agreement with this result, elemental analysis (Table 1) of the EN-MIL-100(Cr) sample shows the incorporation of 2 amine molecules per trimer, which corresponds to one amine molecule per available open metal center,⁵⁴ and demonstrates the effectiveness of the amine grafting process. The IR spectrum of CO

adsorbed on the MMEN-MIL-100(Cr) sample shows an IR absorption band in the C=O stretching region, like that of MIL-100(Cr), although much less intense, which, together with the amine content determined by elemental analysis (1.7 amine molecules per trimer), proves that, contrary to EN-MIL-100(Cr), amine grafting in MMEN-MIL-100(Cr) leaves a small fraction of open metal centers not coordinated to an amine molecule.

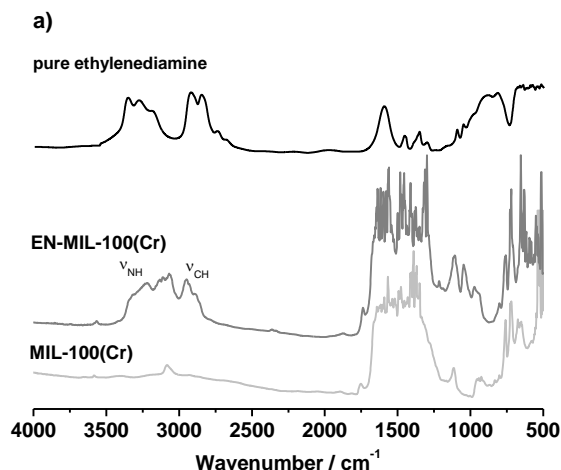


Fig. 3 FTIR spectra of the bare MIL-100(Cr) and the functionalized samples: EN-MIL-100(Cr) (a) and MMEN-MIL-100(Cr) (b) degassed at 423 K. Pure amines (in liquid phase) spectra are shown for comparison.

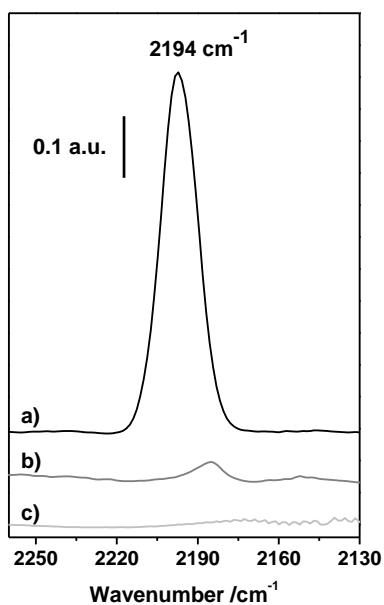


Fig. 4 FTIR spectra of CO adsorbed at 100 K on: a) MIL-100(Cr), b) MMEN-MIL-100(Cr), and c) EN-MIL-100(Cr) samples

Nitrogen adsorption isotherms at 77 K for the three samples are depicted in Figure 5. In agreement with previous results by Ferey et al.,⁴¹ the MIL-100(Cr) nitrogen adsorption isotherm is between type I and IV of the IUPAC classification with two steep rises, at low and high relative pressure, which are indicative of the presence of both micro- and mesopores. BET surface area and pore volume are 1716 m² g⁻¹ and 0.79 cm³ g⁻¹, respectively. Regarding pore size distribution (inset of Figure 5), it shows two maxima, at 20 and 25 Å, corresponding to the small and large cages present in the structure, respectively, in agreement with reported data for other members of the MIL-100 family.⁵⁵⁻⁵⁷ These values, as in previous results,⁵⁵⁻⁵⁷ are underestimated in comparison to van der Waals diameters calculated from crystalline structure. Amine grafted samples show a much reduced nitrogen uptake capacity (Table 1), which may be attributed to grafted amine molecules obstructing nitrogen diffusion as well as to the partial occupation of the space inside the pores. Related to this, pore size distribution curves show that functionalization is also accompanied by a slight decrease of the pore size as expected which suggest that amine groups are directed towards the center of the mesoporous cages.

Table 1. Sample textural properties and nitrogen content

| Sample | S _{BET} (m ² g ⁻¹) | V _p (cm ³ g ⁻¹) | N content* (mmol g ⁻¹) |
|----------------------|--|--|---|
| MIL-100(Cr) | 1716 | 0.79 | - |
| MMEN-MIL- 100(Cr) | 893 | 0.42 | 3.4 (1.7) |
| EN-MIL- 100(Cr) | 484 | 0.22 | 4.2 (2.1) |

* Determined by elemental analysis. Numbers in parentheses denote the content of free amine groups available for CO₂ adsorption.

The adsorption capacity of the amine grafted samples at 308 K and 1 atm of dry CO₂ was gravimetrically evaluated and compared to that of bare MIL-100(Cr). Each sample was first activated at 373 K, then cooled to 308 K under a flow of N₂ prior to exposure to dry CO₂, and the weight change of the adsorbents were followed to determine the adsorption performance of the materials. The results are depicted in Figure 6, which shows that the three sorbents reach their maximum adsorption capacity after about 40 minutes. However, initial adsorption is faster in the case of the amine-grafted samples, especially in the case of EN-MIL-100(Cr), which, after only 2 minutes, adsorbed more than the 50% of its total capacity (to be compared to MIL-100(Cr) which after the same time adsorbed only 0.35 mmol g⁻¹, the 22% of its total capacity). The steeper increase in the case of functionalized materials suggests the presence of binding sites having higher affinity for CO₂ in the case of the functionalized materials. On the other hand, the higher CO₂ adsorption rate of EN-MIL-100(Cr) compared to MMEN-MIL-100(Cr) is likely associated to a more difficult accessibility of CO₂ to secondary amines, due to steric hindrance.^{40,58}

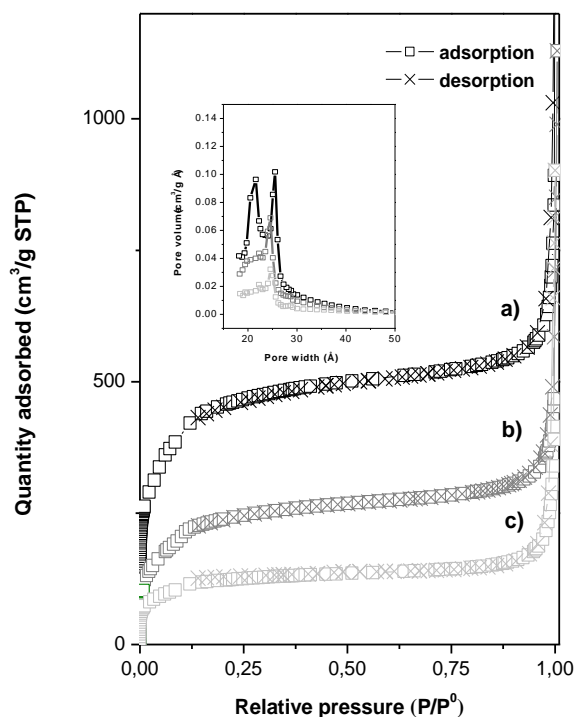


Fig. 5 Nitrogen adsorption-desorption isotherms at 77 K on a) MIL-100(Cr), b) MMEN-MIL-100(Cr), and c) EN-MIL-100(Cr). Square symbols denote adsorption and cross ones desorption. Inset: Corresponding pore size distribution curves calculated using BJH method.

The total amount of CO₂ adsorbed at 308 K on the amine grafted samples was 1.7 mmol g⁻¹ and 2.4 mmol g⁻¹ for MMEN-MIL-100(Cr) and EN-MIL-100(Cr), respectively, which represents a 6% and 50% improvement relative to MIL-100(Cr) (1.6 mmol g⁻¹), showing that, despite the significantly reduced surface area and pore volume with respect to the parent structure, amine grafted samples have a higher CO₂ uptake capacity than the bare MIL-100(Cr) sample, the difference being especially important in the case of EN-MIL-100(Cr). These results indicate that the grafting process improve both, the adsorption capacity and the adsorption kinetics, probably as a consequence of the introduction of additional sites with strong affinity to CO₂ in the samples and that, in this case, the textural properties (pore volume and surface area) contribute but do not have a dominating role in the CO₂ uptake. The fact that CO₂ uptake increases after amine functionalization while N₂ uptake decreases (especially in the case of ethylenediamine functionalized sample) also suggests that functionalization with amino groups also improves the selectivity towards CO₂. Although amine sterics probably also play a role in the different adsorption capacities shown by functionalized materials, predicting its influence in this case is not straightforward because of the difference in amine loadings, being the better results obtained for EN-MIL-100(Cr) sample probably due to the higher degree of functionalization reached in this case.

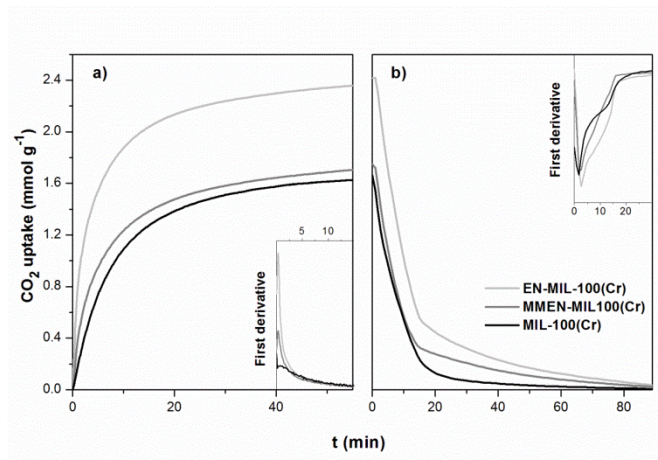


Fig. 6 CO₂ adsorption uptake and kinetics of MIL-100(Cr), MMEN-MIL-100(Cr) and EN-MIL-100(Cr) (a) and their desorption behaviour under N₂ at 373 K (b). Inset: First derivative of the CO₂ adsorption (a) and desorption (b) curves

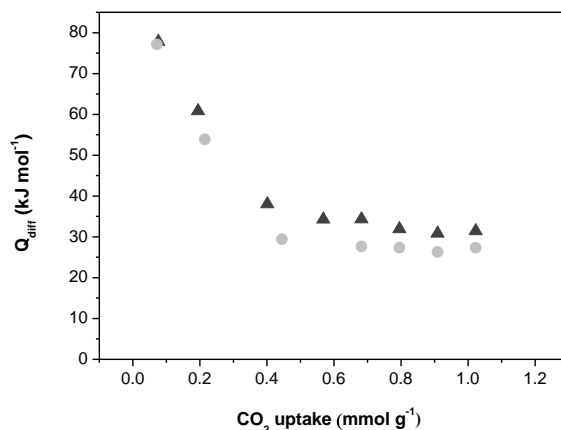


Fig. 7 Differential heats of adsorption as a function of CO₂ uptake for: MMEN-MIL-100(Cr) (squares) and EN-MIL-100(Cr) (circles).

In a previous work,⁵⁹ we obtained, by variable-temperature infrared spectroscopy, an initial standard adsorption enthalpy for carbon dioxide in MIL-100(Cr) of 63 kJ mol⁻¹; value which was in excellent agreement with a previous one reported by Férey et al.⁴⁸ Corresponding data for amine-functionalized samples, determined by microcalorimetry, are shown in Figure 7. The heat of carbon dioxide adsorption of EN-MIL-100(Cr) and MMEN-MIL-100(Cr) approaches 80 kJ mol⁻¹ at zero coverage, a value nearly 20 kJ mol⁻¹ higher than that obtained for MIL-100(Cr), which suggests a strong and selective interaction of CO₂ with the alkylamines functionalities, and compares well with previously reported data obtained for other alkylamine-functionalized metal-organic frameworks.^{31,33,38-40} This high binding energy for CO₂ in amine-functionalized metal-organic frameworks must be attributed to a chemisorptive type interaction, akin to the chemisorption mechanisms that are operative for CO₂ separation using aqueous alkanolamines. The adsorption heat decreases rapidly with increasing loading, indicating that the number of amine groups that strongly adsorb CO₂ is considerable less than the total number of amine molecules grafted to the framework. A similar rapid decrease in the adsorption heat with loading has been reported by other authors and ascribed to the fact that not all of the amine groups are accessible or properly oriented

to react with CO₂.^{33,39,40} Consequently, these results suggest that the improved CO₂ uptake of

functionalized materials (compared with the non-functionalized ones) is not only borne out by the magnitude of the adsorption heat, which is approximately the same for all the samples at loadings higher than 0.5 mmol g^{-1} , but, probably the initial chemisorption interaction between CO_2 and the amine sites facilitates subsequent CO_2 sorption into the framework, as well as co-adsorption of CO_2 molecules.³⁹

Solid sorbents with high adsorption enthalpies have the advantages of high selectivity and capacity but material regeneration is a concern.^{40,60} To ensure the regenerability of the materials, we further performed some regeneration and CO_2 adsorption cycling measurements using a combined temperature swing and nitrogen purge approach. Following activation of the material, a flow of CO_2 was introduced into the furnace at 308 K for 60 minutes. The material was subsequently regenerated with a pure nitrogen purge for 90 min.

For all of the samples, complete CO_2 regeneration is never attained at room temperature being necessary to heat the sample to reach it. As shown in Figure 6b, time for complete regeneration was higher in the case of the functionalized samples which is probably related to the higher heat of adsorption as the regeneration conditions of a CO_2 capture material are expected to depend on the thermodynamics of the adsorption process. Note, however, that in all cases most of the total adsorption capacity is recovered after only 10 minutes at 373 K and that the first derivative of the raw data (inset of Figure 6b) indicate that the rate of desorption is slightly faster in the case of EN-MIL-100(Cr).

The stability and cyclability of the prepared materials as CO_2 adsorbents was tested by repeating the above described procedure 15 times. Results are summarized in Figure 8. It can be observed that after 15 cycles the CO_2 adsorption capacity of MIL-100(Cr) was retained. In the case of MMEN-MIL-100(Cr) and EN-MIL-100(Cr) samples, a complete regeneration of the material was never reached, suggesting that part of the sites may require slightly more forcing conditions to be regenerated. Aside from the incomplete regeneration, the amount of CO_2 adsorbed remains more or less stable during the cycling measurements. After 15 cycles, the total CO_2 adsorption capacity of the functionalized samples is approximately 92% of their maximum adsorption capacity.

Robust long-term stability is important for practical CO_2 capture applications. To evaluate that, the CO_2 adsorption experiments were repeated on the three materials four times over a 6 month period being the final capture uptake $2.2 \pm 0.1 \text{ mmol g}^{-1}$ for EN-MIL-100(Cr), $1.6 \pm 0.1 \text{ mmol g}^{-1}$ for MMEN-MIL-100(Cr), and $1.5 \pm 0.1 \text{ mmol g}^{-1}$ for MIL-100(Cr). The results show that CO_2 adsorption capacity of the three samples undergoes very small changes during this period of time

despite that, between the different series of measurements, the samples were exposed to air and stored under ambient conditions (average relative humidity of 50% and room temperature), thus demonstrating their high stability.

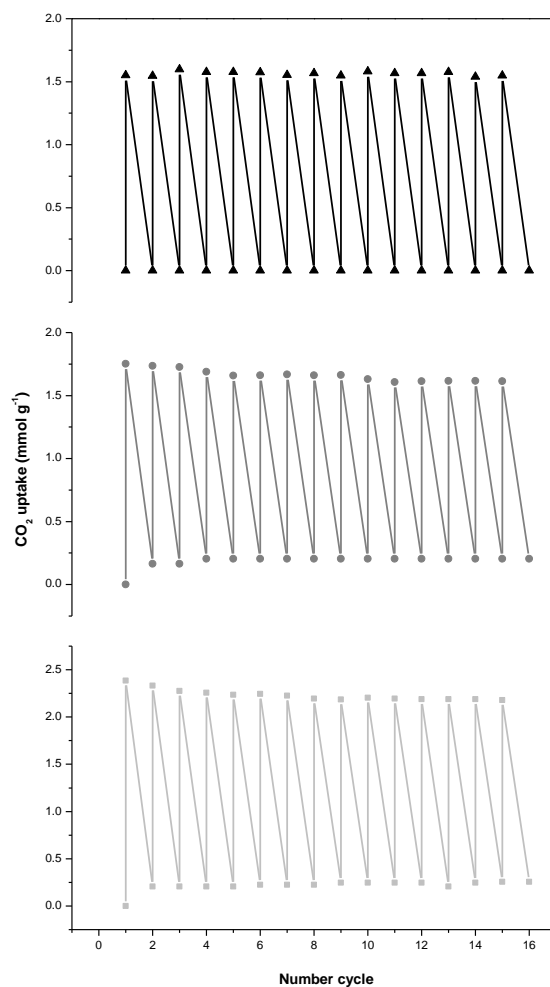


Fig. 8 CO₂ adsorption cycles for MIL-100(Cr) (triangles), MMEN-MIL-100(Cr) (circles), and EN-MIL-100(Cr) (squares) (Pure CO₂ adsorption at 308 K and desorption at 373 K under pure N₂ purge).

Conclusions

In summary, we have shown that functionalization of the MIL-100(Cr) metal-organic framework with alkylamines (ethylenediamine and N,N'-dimethylethylenediamine) results in a substantial increase of CO₂ adsorption heat and adsorption capacity. In particular, ethylenediamine functionalized MIL-100(Cr) showed a CO₂ adsorption capacity of 2.4 mmol g⁻¹ and an adsorption heat of 80 kJ mol⁻¹, to be compared with 1.6 mmol g⁻¹ and 63 kJ mol⁻¹ for MIL-100(Cr). In addition, we found that the amine functionalized MOFs show good stability, even in ambient conditions, fast

adsorption-desorption kinetics and recyclability; as well as high selectivity of CO₂ adsorption (compared to N₂ adsorption), which are desirable properties for porous sorbents for carbon dioxide capture and storage.

Acknowledgments

Financial support from “Programa Pont la Caixa per a grups de recerca de la UIB”, Compagnia di San Paolo and University of Turin (for Project ORTO114XNH through “Bando per il finanziamento di progetti di ricerca di Ateneo - anno 2011”) and European COST Action MP1202 (“Rational design of hybrid organic inorganic interfaces: the next step towards advanced functional materials”) is gratefully acknowledged. C.P.C. acknowledges the support from the Spanish Ministerio de Educación y Ciencia (pre-doctoral fellowship). The authors acknowledge C. Otero Areán for fruitful discussions.

References

- 1 A.W.C. van der Berg and C. Otero Areán, *Chem. Commun.*, 2008, **6**, 668–681.
- 2 R.B. Alley, T. Berntsen, N.L. Bindoff, Z. Chen, A. Chidthaisong, P. Friedlingstein, J.M. Gregory, G.C. Hegerl, M. Heimann, B. Hewitson, B.J. Hoskins, F. Joos, J. Jouzel, V. Kattsov, U. Lohmann, M. Manning, T. Matsuno, M. Molina, N. Nicholls, J. Overpeck, D. Qin, G. Raga, V. Ramaswamy, J. Ren, M. Rusticucci, S. Solomon, R. Somerville, T.F. Stocker, P.A. Stott, R.J. Stouffer, P. Whetton, R.A. Wood and D. Wratt, *Summary for Policymakers, in Climate Change: The Physical Science Basis*, S. Solomon, D. Qin, M. Manning, Z. Chen, M. Marquis, K.B. Averyt, M. Tignor, H.L. Miller eds., Cambridge University Press, Cambridge, 2007.
- 3 F.M. Orr Jr., *Energy Environ. Sci.*, 2009, **2**, 449–458.
- 4 R.S. Haszeldine, *Science*, 2009, **325**, 1647–1652.
- 5 S. Rackley, *Carbon Capture and Storage*, Elsevier, Burlington, Oxford, UK, 2010.
- 6 C.W. Jones and E.J. Maginn, *ChemSusChem*, 2010, **3**, 861–991.
- 7 E.S. Rubin, H. Mantripragada, A. Marks, P. Versteeg and J. Kitchin, *Prog. Energy Combust. Sci.*, 2012, **38**, 630–671.
- 8 M.E. Boot-Handford, J.C. Abanades, E.J. Anthony, M.J. Blunt, S. Brandani, N. Mac Dowell, J.R. Fernández, M.-C. Ferrari, R. Gross, J.P. Hallett, R.S. Haszeldine, P. Heptonstall, A. Lyngfelt, Z. Makuch, E. Mangano, R.T.J. Porter, M. Pourkashanian, G.T. Rochelle, N. Shah, J.G. Yao and P.S. Fennell, *Energy Environ. Sci.*, 2014, **7**, 130–189.
- 9 G.T. Rochelle, *Science*, 2009, **325**, 1652–1654.
- 10 J. Davison, *Energy*, 2007, **32**, 1163–1176.
- 11 K.Z. House, C.F. Harvey, M.J. Aziz and D.P. Schrag, *Energy Environ. Sci.*, 2009, **2**, 193–205.
- 12 E.J. Stone, J.A. Lowe and K.P. Shine, *Energy Environ. Sci.*, 2009, **2**, 81–91.
- 13 M. Nainar, A. Veawab, *Energy Procedia*, 2009, **1**, 231–235.
- 14 A. Pulido, M.R. Delgado, O. Bludsky, M. Rubes, P. Nachtigall and C.O. Areán, *Energy Environ. Sci.*, 2009, **2**, 1187–1195.
- 15 D.M. D’Alessandro, B. Smit and J.R. Long, *Angew. Chem. Int. Ed.*, 2010, **49**, 6058–6082.

- 16 Q. Wang, J. Luo, Z. Zhong and A. Borgna, *Energy Environ. Sci.*, 2011, **4**, 42–55.
- 17 T.C. Drage, C.E. Snape, L.A. Stevens, J. Wood, J. Wang, A.I. Cooper, R. Dawson, X. Guo, C. Satterley and R. Irons, *J. Mater. Chem.*, 2012, **22**, 2815–2823.
- 18 L. Grajciar, J. Cejka, A. Zukal, C. Otero Areán, G. Turnes Palomino and P. Nachtigall, *ChemSusChem*, 2012, **5**, 2011–2022.
- 19 P.D.C. Dietzel, V. Besikiotis and R. Blom, *J. Mater. Chem.*, 2009, **19**, 7362–7370.
- 20 H.J. Park and M.P. Suh, *Chem. Sci.*, 2013, **4**, 685–690.
- 21 A. Schneemann, S. Henke, I. Schwedler and R.A. Fischer, *ChemPhysChem*, 2014, **15**, 823–839.
- 22 B. Li, H. Wang and B. Chen, *Chem. Asian J.*, 2014, **9**, 1474–1498.
- 23 R. Zou, A.I. Abdel-Fattah, H. Xu, Y. Zhao and D.D. Hickmott, *CrystEngComm*, 2010, **12**, 1337–1353.
- 24 J.M. Simmons, H. Wu, W. Zhou and T. Yildirim, *Energy Environ. Sci.*, 2011, **4**, 2177–2185.
- 25 Y.-S. Bae and R.Q. Snurr, *Angew. Chem. Int. Ed.*, 2011, **50**, 11586–11596.
- 26 J. Liu, P.K. Thallapally, B.P. McGrail, D.R. Brown and J. Liu, *Chem. Soc. Rev.*, 2012, **41**, 2308–2322.
- 27 K. Sumida, D.L. Rogow, J.A. Mason, T.M. McDonald, E.D. Bloch, Z.R. Herm, T.-H. Bae and J.R. Long, *Chem. Rev.*, 2012, **112**, 724–781.
- 28 Y. Liu, Z.U. Wang and H.-C. Zhou, *Greenhouse Gas Sci. Technol.*, 2012, **2**, 239–259.
- 29 B. Arstad, H. Fjellvåg, K.O. Kongshaug, O. Swang and R. Blom, *Adsorption*, 2008, **14**, 755–762.
- 30 S. Couck, J.F.M. Denayer, G.V. Baron, T. Rémy, J. Gascon, and F. Kapteijn, *J. Am. Chem. Soc.*, 2009, **131**, 6326–6327.
- 31 A. Demessence, D.M. D’Alessandro, M.L. Foo and J.R. Long, *J. Am. Chem. Soc.*, 2009, **131**, 8784–8786.
- 32 R. Vaidhyanathan, S.S. Iremonger, G.K.H. Shimizu, P.G. Boyd, S. Alavi and T.K. Woo, *Science*, 2010, **330**, 650–653.
- 33 T.M. McDonald, D.M. D’Alessandro, R. Krishna and J.R. Long, *Chem. Sci.*, 2011, **2**, 2022–2028.
- 34 T.M. McDonald, W.R. Lee, J.A. Mason, B.M. Wiers, C.S. Hong and J.R. Long, *J. Am. Chem. Soc.*, 2012, **134**, 7056–7065.
- 35 C. Montoro, E. Gargía, S. Calero, M.A. Pérez-Fernández, A.L. López, E. Barea and J.A.R. Navarro, *J. Mater. Chem.*, 2012, **22**, 10155–10158.
- 36 X. Wang, H. Li and X.-J. Hou, *J. Phys. Chem. C.*, 2012, **116**, 19814–19821.
- 37 H.-L. Jiang, D. Feng, T.-F. Liu, J.-R. Li and H.-C. Zhou, *J. Am. Chem. Soc.*, 2012, **134**, 14690–14693.
- 38 S.-N. Kim, S.-T. Yang, J. Kim, J.-E. Park and W.-S. Ahn, *CrystEngComm*, 2012, **14**, 4142–4147.
- 39 A. Das, M. Choucair, P.D. Southon, J.A. Mason, M. Zhao, C.J. Kepert, A.T. Harris, D.M. D’Alessandro, *Microporous Mesoporous Mater.*, 2013, **174**, 74–80.
- 40 W.R. Lee, S.Y. Hwang, D.W. Ryu, K.S. Lim, S.S. Han, D. Moon, J. Choi and Ch.S. Hong, *Energy Environ. Sci.*, 2014, **7**, 744–751.
- 41 G. Férey, C. Serre, C. Mellot-Draznieks, F. Millange, S. Surblé, J. Dutour and I. Margiolaki, *Angew. Chem.*, 2004, **116**, 6450–6456; *Angew. Chem. Int. Ed.*, 2004, **43**, 6296–6301.
- 42 K.A. Cychosz and A.J. Matzger, *Langmuir*, 2010, **26**, 17198–17202.
- 43 I.Y. Skobelev, K.A. Kovalenko, A.B. Sorokin, V.P. Fedin and O.A. Kholdeeva, *Proceedings of 11th European Congress on Catalysis (EuropaCat-XI)*, Lyon, France, 2013.
- 44 G. Férey, C. Mellot-Draznieks, C. Serre, F. Millange, J. Dutour, S. Surblé and I. Margiolaki, *Science*, 2005, **309**, 2040–2042.
- 45 Y.-K. Seo, J.W. Yoon, J.S. Lee, Y.K. Hwang, C.-H. Jun, J.-S. Chang, S. Wuttke, P. Bazin, A. Vimont, M. Daturi, S. Bourrelly, P.L. Llewellyn, P. Horcajada, C. Serre and G. Férey, *Adv. Mater.*, 2012, **24**, 806–810.
- 46 Q. Liu, L. Ning, S. Zheng, M. Tao, Y. Shi and Y. He, *Scientific Reports* 2013, **3**, 2916.
- 47 I.Y. Skobelev, A.B. Sorokin, K.A. Kovalenko, V.P. Fedin and O.A. Kholdeeva, *J. Catal.*, 2013, **298**, 61–69.

- 48 P.L. Llewellyn, S. Bourrelly, C. Serre, A. Vimont, M. Daturi, L. Hamon, G. De Weireld, J.-S. Chang, D.-Y. Hong, Y.K. Hwang, S.H. Jhung and G. Férey, *Langmuir*, 2008, **24**, 7245–7250.
- 49 Y.K. Hwang, D.Y. Hong, J.S. Chang, S.H. Jhung, Y.-K. Seo, J. Kim, A. Vimont, M. Daturi, C. Serre and G. Férey, *Angew. Chem. Int. Ed.*, 2008, **47**, 4144–4148.
- 50 A. Cauvel, D. Brunel, F. Di Renzo, E. Garrone and B. Fubini, *Langmuir*, 1997, **13**, 2773–2778.
- 51 B. Bonelli, B. Onida, J.D. Chen, A. Galarneau, F. Di Renzo, F. Fajula, B. Fubini and E. Garrone, *Microporous Mesoporous Mater.*, 2006, **87**, 170–176.
- 52 K. Krishnan and R.A. Plane, *Inorg. Chem.*, 1966, **5**, 852–857.
- 53 D.A. Young, T.B. Freedman, E.D. Lipp and L.A. Nafie, *J. Am. Chem. Soc.*, 1986, **108**, 7255–7263.
- 54 A. Vimont, J.-M. Goupil, J.-C. Lavalley, M. Daturi, S. Surblé, C. Serre, F. Millange, G. Férey and N. Audebrand, *J. Am. Chem. Soc.*, 2006, **128**, 3218–3227.
- 55 R. Canioni, C. Roch-Marchal, F. Sécheresse, P. Horcajada, C. Serre, M. Hardi-Dan, G. Férey, J.-M. Grenèche, F. Lefebvre, J.-S. Chang, Y.-K. Hwang, O. Lebedev, S. Turner and G. Van Tendello, *J. Mater. Chem.*, 2011, **21**, 1226–1233.
- 56 Y.-T. Li, K.-H. Cui, J. Li, J.-Q. Zhu, X. Wang and Y.-Q. Tiau, *Chinese J. Inorg. Chem.*, 2011, **27**, 951–956.
- 57 J. Shi, S. Hei, H. Liu, Y. Fu, F. Zhang, Y. Zhong and W. Zhu, *J. Chem.*, 2013, 792827.
- 58 S.A. Didas, A.R. Kulkarni, D.S. Sholl, and C.W. Jones, *ChemSusChem*, 2012, **5**, 2058–2064.
- 59 C. Palomino Cabello, P. Rumori and G. Turnes Palomino, *Microporous Mesoporous Mater.*, 2014, **190**, 234–239.
- 60 W. Lu, J.P. Sculley, D. Yuan, R. Krishna, Z. Wei and H.-C. Zhou, *Angew. Chem., Int. Ed.*, 2012, **51**, 7480–7584.